

NO reduction with NH_3 over chromia–vanadia catalysts supported on TiO_2 : an in situ Raman spectroscopic study

I. Giakoumelou^a, Ch. Fountzoula^b, Ch. Kordulis^b, S. Boghosian^{a,*}

^a Department of Chemical Engineering, University of Patras and FORTH/ICE-HT, Patras, Greece

^b Department of Chemistry, University of Patras and FORTH/ICE-HT, Patras, Greece

Abstract

In situ Raman spectroscopy was used for studying the ternary 2% CrO_3 –6% $\text{V}_2\text{O}_5/\text{TiO}_2$ catalyst, for which a synergistic effect between vanadia and chromia leads to enhanced catalytic performance for the selective catalytic reduction (SCR) of NO with NH_3 . The structural properties of this catalyst were studied under $\text{NH}_3/\text{NO}/\text{O}_2/\text{N}_2/\text{SO}_2/\text{H}_2\text{O}$ atmospheres at temperatures up to 400 °C and major structural interactions between the surface chromia and vanadia species are observed. The effects of oxygen, ammonia, water vapor and sulfur dioxide presence on the in situ Raman spectra are presented and discussed. © 2002 Elsevier Science B.V. All rights reserved.

Keywords: In situ Raman spectroscopy; Chromia and vanadia; Selective catalytic reduction

1. Introduction

Titania-supported vanadia catalysts are used industrially for the selective catalytic reduction (SCR) of NO by NH_3 in the presence of O_2 [1]. The literature abounds in studies related to catalytic activity, effects of vanadia loading, effects of the support nature, kinetics, attempts to elucidate the SCR reaction path and mechanism, etc., but the rate determining step and the structural characteristics of the *active* vanadia site still remain to be realized and continue to be under debate. The plethora of these studies has recently been reviewed [2].

On a subject more closely related to the present article, during the last decade the use of in situ real-time vibrational spectroscopy (mainly Raman) has led to significant progress on the understanding of the structural properties of surface vanadia species [3–8].

The influence of specific oxide supports and metal oxide additives as active phase promoters has been specially examined [7,8].

Of particular interest appears to be the renewed emphasis on studies of $\text{V}_2\text{O}_5/\text{TiO}_2$ catalysts during SO_2 oxidation [9,10] and/or in the presence of SO_2 and H_2O [11]. The undesired SO_2 oxidation occurs simultaneously with the SCR of NO and the structural, redox and catalytic activity properties are greatly affected by the presence of SO_2 , SO_3 and H_2O , which lead to sulfation of the catalyst surface [12,13].

On the other hand, CrO_3 -based catalysts are used in processes such as ethylene polymerization ($\text{CrO}_3/\text{SiO}_2$) and hydrogenation/dehydrogenation of hydrocarbons ($\text{CrO}_3/\text{Al}_2\text{O}_3$) [14]. $\text{CrO}_3/\text{TiO}_2$ catalysts are shown to be promising for low temperature SCR operation and the effect of chromium loading on their activity and physicochemical properties has been addressed [15–17].

Recently, we have been concerned with the structural properties of different forms of vanadia and

* Corresponding author.

E-mail address: boghosian@iceht.forth.gr (S. Boghosian).

chromia in binary V_2O_5/TiO_2 and CrO_3/TiO_2 as well as in ternary $V_2O_5-CrO_3/TiO_2$ catalysts used for the SCR of NO with NH_3 in the presence of O_2 , SO_2 and H_2O . The purposes of our work are: (1) to study the structural properties of the various species by in situ Raman spectroscopy at temperatures up to $400^\circ C$; (2) to establish the effect of catalyst composition on the systematics of the structural and vibrational properties of the species present; (3) to investigate the effect of the presence of SO_2 , O_2 and H_2O in the in situ Raman spectra. Our endeavors to achieve the above are reported elsewhere [18]. The present article is concerned with the in situ Raman study of a ternary $V_2O_5-CrO_3/TiO_2$ catalyst, for which it has recently been established [19] that a cooperation (synergy) between vanadia and chromia active phases leads to enhanced catalytic performance for the SCR of NO with NH_3 in excess O_2 . The structural properties of this catalyst are studied and the effect of the feed gas composition (NH_3 , NO, O_2 , SO_2 and H_2O) on the in situ Raman spectra is discussed. To our knowledge, this is the first in situ Raman study of DeNO_x catalysts, in which the effect of the presence of SO_2 , O_2 and H_2O (or mixtures of these) in the feed gas is examined.

2. Experimental

2.1. Catalyst preparation and characterization

The preparation of the catalysts used in this study has been described elsewhere [19]. The samples are shown in Table 1, and are denoted as $TiCr_xV_y$, where x and y show the content of chromium and vanadium, respectively, expressed in mole percent. It should briefly be stated that deposition of vanadia for preparing the mixed (ternary) $TiCr_2V_6$ catalyst was done by using the $TiCr_2V_0$ sample as precursor, following the deposition of chromia on TiO_2 . Measurements for specific

surface area and pore volume were performed on a Micromeritics ASAP 2000 apparatus, at $-196^\circ C$ with N_2 as adsorption gas. The results are also shown in Table 1.

2.2. In situ Raman spectroscopy

Approximately 100–200 mg of the catalysts were pressed into self-supporting wafers. The catalyst wafer is mounted on a stainless steel adjustable holder in the center of the in situ Raman furnace, which is a kanthal wound double-wall quartz glass tube furnace mounted on a xyz plate and is described in detail elsewhere [18]. Temperature can be controlled with a thermocouple placed inside the holder, near the catalyst. The gases used were O_2 (L'Air Liquide 99.995% purity), 10,000 ppm NH_3/N_2 and NO/ N_2 mixtures (L'Air Liquide), 13,000 ppm SO_2/N_2 mixture (Union Carbide), 4.3% H_2/N_2 mixture (L'Air Liquide) and N_2 (L'Air Liquide 99.999%) as a balance gas and were mixed by using electronic mass flowmeters (Brooks Instr. Model 5850E).

The gas feed consisted of 2000 ppm NO, 2200 ppm NH_3 (ratio $NH_3/NO = 1.1$), 2000 ppm SO_2 , 2% O_2 and 4.3% H_2 balanced in N_2 or various mixtures of these at a total feed flow rate of $50\text{ cm}^3/\text{min}$. In order to study the effect of H_2O vapors in the in situ Raman spectra, the dry feed gas could be bubbled to saturation through water, which was contained in two flasks connected in series and immersed in a thermostat resulting in 3% H_2O vapor content. The outlet gas is passed through a water-cooled jacketed Pyrex glass vessel containing a dilute H_2SO_4 aqueous solution for trapping SO_3 , which is formed in the Raman furnace when SO_2 and O_2 are present in the feed gas.

Raman spectra were excited using the 488.0 nm line of an Ar^+ ion laser (Spectra Physics Model 164), which was focused on the catalytic wafer by a cylindrical lens. The power of the incident light was adjusted

Table 1

Composition, BET specific surface area and pore volume of studied catalyst samples

Catalyst	Ti:Cr:V (atomic ratio)	V_2O_5 (wt.%)	Cr_2O_3 (wt.%)	S_{BET} ($\text{m}^2\text{ g}^{-1}$)	PV ($\text{cm}^3\text{ g}^{-1}$)
TiO_2	100:0:0	0.0	0.0	69.6	0.361
$TiCr_0V_6$	94:0:6	6.9	0.0	42.4	0.297
$TiCr_2V_0$	98:2:0	0.0	1.9	61.0	0.339
$TiCr_2V_6$	92:2:6	6.8	1.9	51.0	0.285

at 120 mW. The scattered light was collected at 90° (horizontal scattering plane), analyzed with a 0.85 m Spex 1403 double monochromator and detected by a –20 °C cooled RCA photomultiplier equipped with EG&G photon counting electronics.

Recording of spectra started typically at 100 °C in N₂, and then each sample was oxidized for 1 h at 400 °C in O₂. Raman spectra were then recorded successively in O₂, NH₃/N₂, NH₃/NO/N₂, NH₃/NO/O₂/N₂, O₂/N₂/H₂O, SO₂/N₂, SO₂/O₂/N₂ and SO₂/O₂/H₂O/N₂ at 400, 250 and 100 °C, after 1 h of gas treatment. In some occasions (e.g. to check the case of slow reduction rate) the gas treatment was extended up to ~12 h.

3. Results and discussion

3.1. Catalyst composition effects and structural properties

Fig. 1 shows in situ Raman spectra taken at 400 °C during exposure to O₂ for TiO₂ (a), TiCr₀V₆ (b), TiCr₂V₀ (c) and TiCr₂V₆ (d). All spectra are recorded after 1 h of exposure of the catalysts to flowing O₂ at 400 °C (dehydrated conditions). Spectrum (b) of the 6% V₂O₅/TiO₂ catalyst (TiCr₀V₆) shows that vanadia is present in the form of: (1) monomeric mono-oxo vanadyl species with the characteristic V=O stretch at 1029 cm⁻¹ [3,4] possessing probably a distorted tetrahedral configuration with three V–O–Ti bonds anchored to the surface [9,20]; (2) oligomeric or polymeric vanadates with characteristic terminal V=O stretches of vanadyl groups internal to polymeric units and dioxo-vanadium groups terminating the chains [3,9], which give rise to the broad feature in the 915–960 cm⁻¹ region; (3) crystalline V₂O₅ with a characteristic band at 994 cm⁻¹, which indicates that monolayer coverage is exceeded for this sample. The broadness of the 915–960 cm⁻¹ feature due to V=O stretchings of polymeric vanadates can be accounted for by variations in the number of V–O–Ti anchoring bonds per vanadium atom, which combined with possible variations in the CN (coordination number) of vanadium results in a distribution of related configurations with different V–O bond strengths. The band at 1013 cm⁻¹ is attributed to V=O terminal stretches of monomeric (Ti–O)₃V=O

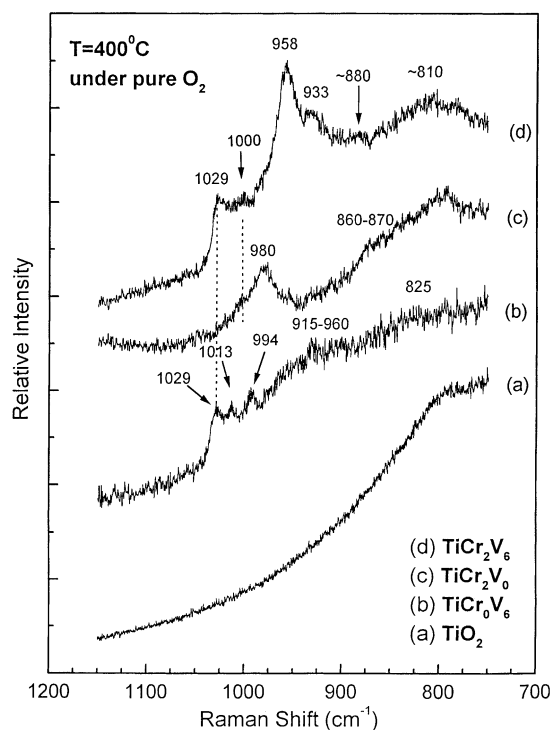


Fig. 1. In situ Raman spectra of: (a) TiO₂ support; (b) TiCr₀V₆; (c) TiCr₂V₀; (d) TiCr₂V₆ catalysts under O₂ at 400 °C. Laser wavelength, $\lambda_0 = 488.0$ nm; laser power, $w = 120$ mW; spectral slit width, $ssw = 7$ cm⁻¹.

species in close proximity to each other caused by the high vanadia loading (6%), which results in mutual repulsion of the terminal oxygens and weakens the corresponding V=O bonds, giving rise to the 1013 cm⁻¹ band [3]. Finally, the 825 cm⁻¹ broad band is assigned to V–O–V vibrations. Spectrum (c) of the 2% CrO₃/TiO₂ catalyst is characterized by bands at 980 cm⁻¹ (with a weak shoulder at ~1000 cm⁻¹) corresponding to terminal Cr=O vibrations of the surface chromia species, while a broad band centered around 860 cm⁻¹ due to Cr–O–Cr vibrations indicates the existence of polychromate species. Increase of chromia loading results in increase of the 1000 and 860 cm⁻¹ bands indicating that they both originate from the same species, namely from oligomeric dehydrated polychromates, whereas the 980 cm⁻¹ band is assigned to isolated dehydrated monochromate. The above assignments are in perfect agreement with the spectroscopic fingerprints of supported Cr species

[21]. The dehydrated monochromate probably possesses two Cr=O terminal bonds (di-oxo species) judged from the 980 cm^{-1} Cr=O band position, which is very close to the respective value reported for the CrO_2Cl_2 reference compound [22]. Finally, the spectrum of the ternary 2% CrO_3 –6% $\text{V}_2\text{O}_5/\text{TiO}_2$ (TiCr_2V_6) catalyst (Fig. 1d) can by no means be considered as a superposition of bands due to the binary TiCr_2V_0 and TiCr_0V_6 samples and shows that major structural interactions take place between the surface chromia and vanadia species, implying the formation of a mixed Cr–O–V surface species. Bands at 1029 , ~ 1000 , 958 and 933 cm^{-1} can be seen in the M=O stretching region and broader bands at 880 and 810 cm^{-1} are observed in the M–O–M stretching region. No band due to crystalline V_2O_5 is observed for TiCr_2V_6 , contrary to the case of the binary TiCr_0V_6 with the same vanadia loading, which possesses the characteristic 994 cm^{-1} band (Fig. 1b).

The 1029 cm^{-1} band is the only band common to the spectra of TiCr_2V_6 and TiCr_0V_6 and is assigned to terminal V=O stretch of isolated mono-oxo vanadyl species possessing a distorted tetrahedral configuration. Therefore, part of vanadia is deposited on the TiCr_2V_0 precursor in the form of isolated mono-oxo tetrahedral vanadyl species. Previously [19], it has been shown that following the second impregnation step for deposition of vanadia, the isolated tetrahedral monochromate transforms into nonterminal chromate in the TiCr_2V_6 catalyst. Therefore, the 1000 cm^{-1} band, which can be seen partly obscured between the 1029 and 958 cm^{-1} bands can be assigned to Cr=O terminal stretch, as expected for chromate groups participating in polymeric or oligomeric chains [21]. The 958 and 933 cm^{-1} bands are also in the M=O stretching region and are assigned to V=O stretching vibrations due to vanadyl groups internal to polymeric units and dioxo-vanadium groups terminating the chains. A number of similar related configurations of V=O terminal bonds appears to exist also in the binary TiCr_0V_6 sample (Fig. 1b), giving rise to the broad 915 – 960 cm^{-1} feature and pointing to existence of at least two kinds of such bonds as described. Furthermore, the existence of surface polymeric V_xO_y units in which vanadium has CN > 4 (i.e. 5 or 6) has not been excluded [3,24].

The sharp and well-resolved appearance of the 958 and 933 cm^{-1} bands in the TiCr_2V_6 spectra com-

pared to the 915 – 960 cm^{-1} broad feature exhibited by TiCr_0V_6 is indicative of “high” order which is in perfect agreement with the active phase deposition mechanism proposed recently for the TiCr_2V_6 catalyst [19]. According to this mechanism, during the second impregnation step for deposition of the vanadia phase on the TiCr_2V_0 precursor, hydrolysis of one of the Ti–O–Cr bonds anchoring the isolated monochromate groups takes place resulting in hydrolyzed Cr^{6+} species associated with the titania surface. This mechanism creates a new adjacent protonated surface hydroxyl group per chromate unit and a portion of vanadia species could be adsorbed on this site, in the vicinity of the partly hydrolyzed isolated chromia units [19]. In this way, not only the consumption of protonated surface hydroxyl sites following the prior deposition of a small loading of Cr (2 mol%) is compensated, but a very good dispersion of vanadia species is also ensured. Finally, the deposition of vanadia species on sites adjacent to the isolated chromate species favors the creation of Cr–O–V bridges during catalyst calcination, thus transforming the above units to nonisolated ones. This is in agreement with the previous assignment of the 1000 cm^{-1} band of the TiCr_2V_6 spectrum (Fig. 1d) to Cr=O vibrations of chromate groups participating in polymeric or oligomeric chains. Furthermore, the 880 cm^{-1} band is assigned to vibrations of Cr–O–V functionalities, whereas the 810 cm^{-1} band is assigned to V–O–V bridging vibrations. In this way, an “ordered decoration” of well dispersed isolated monochromates by vanadia takes place resulting to high coverage and preventing the formation of V_2O_5 crystalline phase contrary to the case of the binary TiCr_0V_6 catalyst where for the same vanadia loading crystalline V_2O_5 is formed (judged by the sharp 994 cm^{-1} band in the Raman spectra of Fig. 1b).

It is noteworthy that such interactions between chromia and vanadia have not been observed in other compositions of the ternary TiCr_xV_y catalysts studied by us [18,19] or others [23]. Dunn et al. [23] have even reached the conclusion that no structural interactions between chromia and vanadia take place but their study was limited only in one composition of the ternary catalyst (5% CrO_3 –1% $\text{V}_2\text{O}_5/\text{TiO}_2$), for which indeed there appears to be no interaction between the surface metal oxide species. Furthermore, it should be pointed out that useful hints for assigning

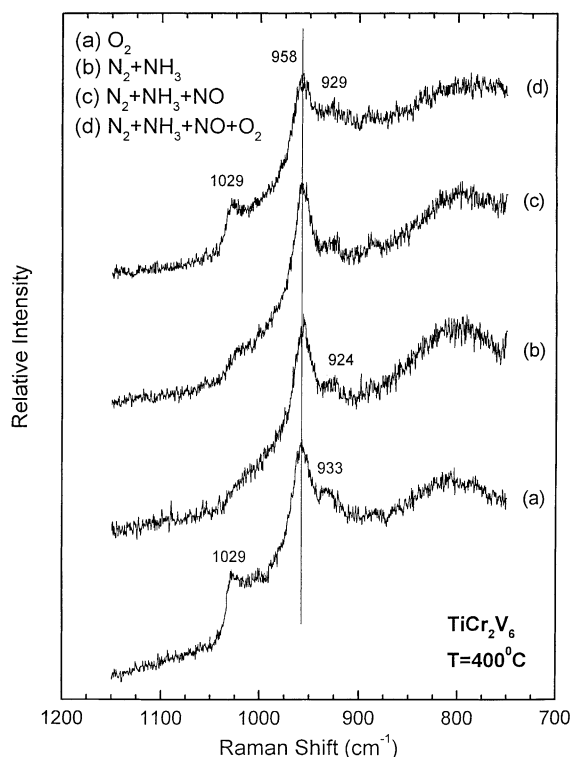


Fig. 2. In situ Raman spectra of TiCr_2V_6 catalyst at 400°C under $\text{O}_2/\text{NH}_3/\text{NO}/\text{N}_2$ atmospheres as listed in the figure. $\lambda_0 = 488.0\text{ nm}$, $w = 120\text{ mW}$ and $\text{ssw} = 7\text{ cm}^{-1}$.

$\text{Me}=\text{O}$ vibrational Raman bands have been proposed also recently, based on DFT calculations for model clusters [25].

3.2. The ternary 2% CrO_3 –6% $\text{V}_2\text{O}_5/\text{TiO}_2$ catalyst under SCR reaction conditions

Fig. 2 shows in situ Raman spectra of the 2% CrO_3 –6% $\text{V}_2\text{O}_5/\text{TiO}_2$ (TiCr_2V_6) catalyst in various $\text{NH}_3/\text{NO}/\text{O}_2/\text{N}_2$ gas atmospheres at 400°C . All spectra are recorded after 1 h of exposure to the atmospheres indicated in the figure. Spectrum (a) is taken under O_2 and represents the fully oxidized state of the catalyst. After 1 h of exposure to NH_3/N_2 the following observations can be made in the in situ Raman spectrum (Fig. 2b): (a) the 1029 cm^{-1} $\text{V}=\text{O}$ band due to isolated vanadyl species broadens and shifts to $\sim 1010\text{ cm}^{-1}$ in agreement with what is observed for binary $\text{V}_2\text{O}_5/\text{TiO}_2$ catalysts [4,18]; (b) the 1000 cm^{-1}

$\text{Cr}=\text{O}$ band can no longer be seen, obscured under the envelope of the band arising from the red (down-scale) shift of the $\text{V}=\text{O}$ band of the isolated vanadyl species; (c) the position and intensity of the 958 cm^{-1} $\text{V}=\text{O}$ band of the polymeric $\text{Cr}-\text{O}-\text{V}$ species remains unaffected; (d) the second $\text{V}=\text{O}$ band of the polymers undergoes a red shift from 933 to 924 cm^{-1} without diminishing in intensity; (e) the bridging features at 880 cm^{-1} ($\text{Cr}-\text{O}-\text{V}$) and 810 cm^{-1} ($\text{V}-\text{O}-\text{V}$) remain unchanged. As can be seen in spectrum (c) of Fig. 2, admission of NO along with NH_3/N_2 does not induce significant changes, except from a partial reappearance of the $\text{V}=\text{O}$ monomeric peak. Finally, as can be seen in Fig. 2d, when O_2 is fed along with $\text{NH}_3/\text{NO}/\text{N}_2$ the spectral features of the fully oxidized catalyst are almost restored. Fig. 2d shows that NH_3 is not completely removed from the polymeric $\text{V}=\text{O}$ species. A more careful inspection of Fig. 2 reveals that the restoration of spectral features of the fully oxidized catalyst had been started since NO was added in the NH_3/N_2 feed (see Fig. 2c). This is explained by taking into account that adsorbed NH_3 reacts with NO and thus its surface concentration is diminished in the presence of NO in the catalyst environment. On the other hand, it is well known that O_2 accelerates the SCR of NO by NH_3 . So, the concentration of adsorbed NH_3 on the $\text{V}=\text{O}$ sites is expected to be further diminished, and in turn the spectral features of the fully oxidized catalyst to be approached, upon O_2 addition in the gas feed. The fact that the 1029 cm^{-1} band attributed to isolated vanadyl species is almost completely restored probably shows that these species are less active than polymeric $\text{V}=\text{O}$ species for the SCR of NO by NH_3 . This is in agreement with the dual-site Eley–Rideal mechanism proposed for the SCR reaction on the vanadia–titania catalysts [26–29]. According to this mechanism, two sites ($\text{V}-\text{OH}$ and $\text{V}=\text{O}$) are needed in order for a catalytic cycle to be completed. Thus, it seems reasonable to suppose that the polymeric vanadia species, which could provide a greater number of such pairs of sites than the isolated monomeric vanadyl species, can retain NH_3 in a higher extent.

In situ Raman spectra of binary $\text{CrO}_3/\text{TiO}_2$ catalysts in NH_3/N_2 atmosphere possess no bands in the $\text{Cr}^{6+}=\text{O}$ stretching region [18] showing that chromate units are susceptible to reduction by NH_3 and the same can be assumed here for the ternary TiCr_2V_6

catalyst. Thus, the broad and weak wing seen around 1010 cm^{-1} in Fig. 2b is due to the down-scale shift, broadening and weakening of the $\text{V}=\text{O}$ monomeric peak as shown earlier [4].

In conclusion, NH_3 reduces Cr^{6+} and causes significant changes in band position and intensity associated with the $\text{V}=\text{O}$ stretch of monomeric vanadyls as well as in the band position associated with one kind of $\text{V}=\text{O}$ stretch of polymeric $\text{Cr}-\text{O}-\text{V}$ species. In the case of the monomeric vanadyl, the changes are attributed to partial reduction of the dispersed isolated vanadia species due to removal of oxygen from $\text{V}=\text{O}$ groups as suggested earlier [4]. The shift of the 933 cm^{-1} $\text{V}=\text{O}$ band of the polymeric chain to 924 cm^{-1} is attributed to perturbations caused by ammonia adsorption/coordination to vanadium. It has been proposed [2] that ammonia can be adsorbed in two different strongly held species in $\text{V}_2\text{O}_5/\text{TiO}_2$ catalysts: (a) molecularly adsorbed NH_3 through Lewis-type interaction on coordinatively unsaturated vanadium; (b) NH_3 adsorbed as ammonium ion over Brønsted acidic $-\text{OH}$ surface hydroxy groups. ^{15}N -NMR experiments allowed to conclude that adsorption on Lewis sites is predominant in $\text{V}_2\text{O}_5/\text{TiO}_2$ [30]. Therefore, the behavior of the 958 and 933 cm^{-1} bands in the presence of NH_3 , where one of them remains unchanged and the other undergoes a 9 cm^{-1} red shift, supports our assignment for these bands to $\text{V}=\text{O}$ terminal stretches of two *different* nonisolated VO_x groups in which the V atoms have different CN and at least one of them is coordinatively unsaturated.

3.3. In situ Raman spectra in the presence of H_2O and SO_2

Fig. 3 shows in situ Raman spectra of the TiCr_2V_6 catalyst in dehydrated conditions at 400°C (a), $\text{H}_2\text{O}/\text{O}_2/\text{N}_2$ atmospheres at 400°C (b), 250°C (c) and 100°C (d). The only changes seen upon exposure to water vapor are associated with a gradual broadening and intensity loss of the 1029 cm^{-1} $\text{V}=\text{O}$ band of the isolated monomeric vanadates, which eventually almost disappears at 100°C (spectrum (d)). Separate runs in the absence of water vapor showed that the observed sharpening and blue (up-scale) shift of the 958 , 933 and 880 cm^{-1} bands with decreasing temperature is not associated with the presence

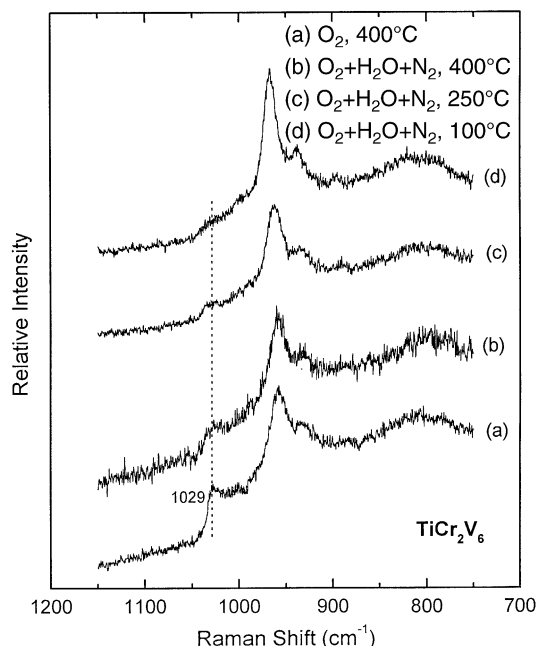


Fig. 3. In situ Raman spectra of TiCr_2V_6 catalyst under: O_2 at 400°C (a); $\text{O}_2/\text{H}_2\text{O}/\text{N}_2$ at 400°C (b); 250°C (c); 100°C (d). $\lambda_0 = 488.0\text{ nm}$, $w = 120\text{ mW}$ and $\text{ssw} = 7\text{ cm}^{-1}$.

of moisture. Thus the effect is attributed mainly to thermal broadening at elevated temperatures. Already at 400°C , the 1029 cm^{-1} $\text{V}=\text{O}$ band loses almost 50% of its intensity indicating that moisture interacts with the dehydrated surface $(\text{Ti}-\text{O})_3\text{V}=\text{O}$ species probably through hydrogen bonding [31]. At lower temperatures the band can hardly be identified and thus the surface isolated vanadate species appear to be “flooded”. However, the observed effects for the studied ternary $\text{CrO}_3-\text{V}_2\text{O}_5/\text{TiO}_2$ catalyst are somewhat different to the previously observed gradual broadening and down-scale shift of the $\text{V}=\text{O}$ monomeric stretch in the presence of water in binary $\text{V}_2\text{O}_5/\text{TiO}_2$ catalysts [31]. Recent in situ Raman spectra of binary $\text{CrO}_3/\text{TiO}_2$ and $\text{V}_2\text{O}_5/\text{TiO}_2$ catalysts in the presence of water vapor [18] show features similar to those reported in [31].

Sulfur dioxide is present in exhaust gases of the power plants and is oxidized to SO_3 over vanadia catalysts but SO_2 oxidation is undesirable during the SCR reaction [9]. Recent studies have addressed: (a) the reactivity of V_2O_5 catalysts for the SCR reaction in the presence of SO_2 and H_2O [11]; (b) the

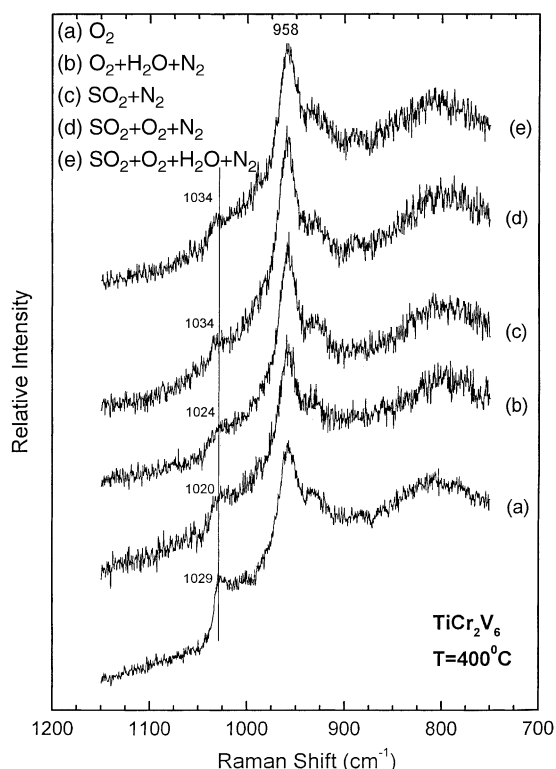


Fig. 4. In situ Raman spectra of TiCr_2V_6 catalyst at 400°C under: (a) O_2 ; (b) $\text{O}_2/\text{H}_2\text{O}/\text{N}_2$; (c) SO_2/N_2 ; (d) $\text{SO}_2/\text{O}_2/\text{N}_2$; (e) $\text{SO}_2/\text{O}_2/\text{H}_2\text{O}/\text{N}_2$. $\lambda_0 = 488.0\text{ nm}$, $w = 120\text{ mW}$ and $\text{ssw} = 7\text{ cm}^{-1}$.

interactions between surface vanadate and sulfate species on sulfated supported vanadia catalysts in dehydrated conditions [13]. Furthermore, molecular structure–reactivity relationships for SO_2 oxidation over supported vanadia catalysts have been reviewed [24].

Fig. 4 shows in situ Raman spectra of the TiCr_2V_6 catalyst at 400°C in: dehydrated conditions (a); $\text{H}_2\text{O}/\text{O}_2/\text{N}_2$ (b); SO_2/N_2 (c); $\text{SO}_2/\text{O}_2/\text{N}_2$ (d); $\text{SO}_2/\text{O}_2/\text{H}_2\text{O}/\text{N}_2$ (e) atmospheres. Spectra (a) and (b) have already been discussed and are included for comparison. Significant changes in the intensity as well as in the position of the 1029 cm^{-1} $\text{V}=\text{O}$ monomeric peak can be observed in spectra (c)–(e) of Fig. 4, whereas all the remaining spectral features are unaffected. In spectrum (c), following exposure to SO_2 , the 1029 cm^{-1} band loses more than 50% of its intensity and undergoes a red (down-scale) shift to

1024 cm^{-1} . The intensity loss is interpreted to indicate reduction in the number of $\text{V}^{5+}=\text{O}$ vibrators of the isolated vanadates due to partial reduction of V^{5+} either to V^{4+} or V^{3+} . The down-scale shift is probably due to perturbations in the $\text{V}=\text{O}$ bond strength caused by adsorbed SO_2 . Previously, Dunn et al. [9] have demonstrated by kinetic studies that the SO_2 oxidation reactivity of supported $\text{V}_2\text{O}_5/\text{TiO}_2$ catalysts is not related to either the terminal $\text{V}=\text{O}$ bond or the presence of $\text{V}-\text{O}-\text{V}$ bridging bonds and proposed that the reaction proceeds through adsorption of SO_2 to the $\text{V}-\text{O}-\text{Ti}$ bond following cleavage of the anchoring $\text{O}-\text{Ti}$ bond. Furthermore, they proposed that the reaction path may involve either a $(\text{V}^{5+})\cdot\text{SO}_2$ or a $(\text{V}^{3+})\cdot\text{SO}_3$ surface complex. However, it remains questionable how easy it is to monitor spectroscopically such catalytically active species in reaction conditions [24].

As seen in Fig. 4, sulfur dioxide does not seem to affect the polymeric species (both the 933 and 958 cm^{-1} bands are not affected). Since these species may be relevant to the catalyst activity for the SCR of NO by NH_3 , it is expected that the activity of the 2% Cr_2O_3 –6% $\text{V}_2\text{O}_5/\text{TiO}_2$ catalyst may remain stable in the presence of SO_2 . Such studies will be undertaken shortly.

Admission of O_2 or O_2 and H_2O vapors along with SO_2 is expected to reestablish vanadium in the +5 oxidation state and results in a blue shift of the $\text{V}=\text{O}$ band of the isolated vanadyl centers to 1034 cm^{-1} as seen in spectra (d) and (e) in Fig. 4. Thus, formation of SO_3 and SO_4^{2-} species appears to strengthen the $\text{V}=\text{O}$ bond probably due to the weaker basic character of SO_4^{2-} ions which act as ligands for coordinatively unsaturated vanadyl centers in sulfated catalysts relative to oxide species of sulfate-free catalysts [10]. Surface anchored SO_4^{2-} species could not be observed, most probably due to the high surface coverage of the 2% Cr_2O_3 –6% $\text{V}_2\text{O}_5/\text{TiO}_2$ catalyst in agreement with an explanation given elsewhere [13].

4. Conclusions

The ternary 2% Cr_2O_3 –6% $\text{V}_2\text{O}_5/\text{TiO}_2$ catalyst, for which a synergistic effect between vanadia and chromia leads to enhanced catalytic performance for the SCR of NO by NH_3 has been studied by in situ

Raman spectroscopy under $\text{NH}_3/\text{NO}/\text{O}_2/\text{N}_2/\text{SO}_2/\text{H}_2\text{O}$ atmospheres at temperatures up to 400°C . The results indicate that: (i) under O_2 at 400°C (dehydrated conditions), the catalyst contains monomeric vanadyl species ($\text{V}=\text{O}$ at 1029 cm^{-1}) and two-dimensional (oligomeric) $\text{Cr}-\text{O}-\text{V}$ chains consisted of nonterminal chromates ($\text{Cr}=\text{O}$ at 1000 cm^{-1}) and oligomeric vanadates ($\text{V}=\text{O}$ at 958 and 933 cm^{-1}); (ii) the ternary catalyst does not contain crystalline V_2O_5 , a fact which indicates the very good dispersion of vanadia (explained by a proposed deposition mechanism leading to an “ordered decoration” of well dispersed monochromates by vanadia); (iii) NH_3 associates to the monomeric vanadyls and to *one* of the polymeric vanadyls (possessing the 933 cm^{-1} band), whereas the spectral behavior under SCR reaction conditions points to the 933 cm^{-1} $\text{V}=\text{O}$ band of the polymers as representing the reactive species; (iv) water vapors affect the monomeric vanadyls preferentially; (v) sulfur dioxide appears to reduce the monomeric vanadyls and leave the polymeric vanadates unaffected.

Acknowledgements

NATO's Scientific Affairs Division in the framework of the Science for Peace Programme (SfP 971984) has sponsored this research. Support from the General Secretariat of Research and Technology of the Greek Ministry of Development and FORTH/ICE-HT is gratefully acknowledged.

References

- [1] H. Bosch, F. Janssen, *Catal. Today* 2 (1988) 369.
- [2] G. Busca, L. Lietti, G. Ramis, F. Berti, *Appl. Catal. B* 18 (1998) 1.
- [3] G. Went, L.-J. Leu, A.T. Bell, *J. Catal.* 134 (1992) 479.
- [4] G. Went, L.-J. Leu, A.T. Bell, *J. Catal.* 134 (1992) 492.
- [5] G. Went, L.-J. Leu, S.J. Lombardo, A.T. Bell, *J. Phys. Chem.* 96 (1992) 2235.
- [6] N.-Y. Topsoe, J.A. Dumesic, H. Topsoe, *J. Catal.* 151 (1995) 241.
- [7] I.E. Wachs, G. Deo, B. Weckhuysen, A. Andreini, M.A. Vuurman, M. de Boer, M.D. Amiridis, *J. Catal.* 161 (1996) 211.
- [8] M.D. Amiridis, R.V. Duevel, I.E. Wachs, *Appl. Catal. B* 20 (1999) 111.
- [9] J.P. Dunn, P.R. Koppula, H.G. Stenger, I.E. Wachs, *Appl. Catal. B* 19 (1998) 103.
- [10] C. Orsenigo, A. Beretta, P. Forzatti, J. Svachula, E. Tronconi, F. Bregani, A. Baldacci, *Catal. Today* 27 (1996) 15.
- [11] M.D. Amiridis, I.E. Wachs, G. Deo, J.-M. Jehng, D.S. Kim, *J. Catal.* 161 (1996) 247.
- [12] C. Orsenigo, L. Lietti, E. Tronconi, P. Forzatti, F. Bregani, *Ind. Eng. Chem. Res.* 37 (1998) 2350.
- [13] J.P. Dunn, J.-M. Jehng, D.S. Kim, L.E. Briand, H.G. Stenger, I.E. Wachs, *J. Phys. Chem. B* 102 (1998) 6212.
- [14] D.S. Kim, I.E. Wachs, *J. Catal.* 142 (1993) 166.
- [15] B.L. Duffy, H.E. Curry-Hyde, N.W. Cant, P.F. Nelson, *J. Catal.* 149 (1994) 11.
- [16] H. Schneider, M. Maciejewski, K. Kohler, A. Wokaum, A. Baiker, *J. Catal.* 157 (1995) 301.
- [17] Ch. Fountzoula, H. Matralis, Ch. Papadopolou, G.A. Voyiatzis, Ch. Kordulis, *J. Catal.* 172 (1997) 391.
- [18] I. Giakoumelou, S. Boghosian, in preparation.
- [19] Ch. Fountzoula, H. Matralis, Ch. Papadopolou, G.A. Voyiatzis, Ch. Kordulis, *J. Catal.* 184 (1999) 5.
- [20] I.E. Wachs, B.M. Weckhuysen, *Appl. Catal. A* 157 (1997) 67.
- [21] B.M. Weckhuysen, I.E. Wachs, R.A. Schoonheydt, *Chem. Rev.* 96 (1996) 3327.
- [22] K. Nakamoto, *Infrared and Raman Spectra of Inorganic and Coordination Compounds*, 4th Edition, Wiley/Interscience, New York, 1986.
- [23] J. Dunn, H.G. Stenger, I.E. Wachs, *J. Catal.* 181 (1999) 233.
- [24] J. Dunn, H.G. Stenger, I.E. Wachs, *Catal. Today* 51 (1999) 301.
- [25] M. Najbar, E. Broclawik, A. Gora, J. Camra, A. Bialas, A. Weselucha-Birczynska, *Chem. Phys. Lett.* 325 (2000) 330.
- [26] A. Miyamoto, T.U.K. Kobayashi, M. Inomata, Y. Murakami, *J. Phys. Chem.* 86 (1982) 2945.
- [27] M. Inomata, A. Miyamoto, Y. Murakami, *J. Catal.* 62 (1980) 140.
- [28] A. Miyamoto, Y. Yamazaki, M. Inomata, Y. Murakami, *J. Phys. Chem.* 85 (1981) 2366.
- [29] N.Y. Topsoe, *Science* 265 (1994) 1217.
- [30] S. Hu, T.M. Apple, *J. Catal.* 158 (1996) 199.
- [31] J.-M. Jehng, G. Deo, B.M. Weckhuysen, I.E. Wachs, *J. Mol. Catal. A* 110 (1996) 41.